Active Galaxies with Compact Jets Studied at RATAN-600

Yu. A. Kovalev[1], G. V. Zhekanis[2], Y. Y. Kovalev[1,3], A. V. Popkov[3,1], A. V. Plavin[1,3], N. A. Nizhelsky[2], P. G. Tsybulev[2], Yu. V. Sotnikova[2], A. K. Erkenov[2], and S. V. Troitsky[4]

[1] Astro Space Center of Lebedev Physical Institute of RAS, Moscow, Russia;
[2] Special Astrophysical Observatory of RAS, Nizhny Arkhyz, Russia;
[3] Moscow Institute of Physics and Technology, Dolgoprudny, Russia;
[4] Institute of Nuclear Researches of RAS, Moscow, Russia

Abstract. Main results are presented from the research program for a sample of active galaxies and quasars with VLBI-compact jets observed with RATAN-600. A joint analysis of RATAN-600 data and ground-based VLBI networks indicated the possibility of dividing the spectra into compact (VLBI core and jet on parsec scales) and extended (magnetized shell around the jet, including kiloparsec "lobes") components. This was verified and implemented using model analysis methods. The results made it possible to select candidates for mass VLBI surveys and help implementation of a modern high-precision inertial reference system. A joint analysis of RATAN-600, VLBI data and the results of high-energy neutrino detection using the IceCube telescope demonstrated the connection of neutrino emitters with radio bursts of active galaxies and localized the region of astrophysical neutrino generation within the central parsecs of active galaxies. A joint analysis of RATAN-600 and RadioAstron data showed that the extreme brightnesses in the jets of active galaxies are observed mainly at the same time or after bursts of radio emission accompanied by changes in the self-absorption conditions in quasar nuclei. Together with the neutrino results, this suggests importance of synchrotron radiation of relativistic protons in the jets of at least some active galaxies.

Keywords: galaxies: active; galaxies: jets; quasars: general; radio continuum: galaxies

DOI:10.26119/978-5-6045062-0-2_2020_355

1 Long-Term Spectra Variability Study

The evolution of the observational program has been shown on the Table 1 per years, including the number of wide-band receivers at the frequencies from 1 to 22 GHz. The typical central wavelenghts during all years are 1.38 (1.35), 2.7, 3.9, 6.2 (7.6, 8.2) 13 and 31 (24) cm. The instantaneous spectrum at these frequencies is measured in a few minutes by the transit mode of RATAN-600 (Korolkov & Pariiskii 1979; Parijskij 1993). For details of observations, processing, and calibration, see Kovalev et al. (1999). The details and results on the first half of the program before 1997 have been discussed in Kovalev (1997).

Goal: investigation of the nature of instantaneous multi-frequency radio spectra of quasars and galaxies and their long-term variability. Objects: extragalactic objects with variable radio emission (since 1979) or with VLBI-compact components (since 1997). The first study of the sample for 550 VLBI objects from Preston et al. (1985) had been started in 1997. Three main tasks and their main results are discussed in next three sections.

Table 1. The program statistics. P – Paper tape recorder; M – Magnetic tape recorder; PC – a computer with Hard Disk; Mera/Mpc – magnetic disk of computer "MERA" or "PC"; S, A, A+F – installing antenna elements of the 1-st reflector: Semi-automatic, Automatic, Automatic with Fixing the results; M – Manual 20-m roulette measuring the focal distances of the 2-nd antenna reflector from one of 8 geodetic reference points.

Years, 1900 +	79–82	82–87	87–92	94–96	97–109	110–113	114–116	117-120
Objects, total	11–16	16–60	115	200	700–4000	1000	700	700–999
Frequencies, total	5–6	6–7	6–7	6	6–13	6–4	4–5	5–6
Sets per a year	4	3–4	3–4	5	4–3	3–4	3–4	6–4
Days per a set	6–20	6–7	6–7	10	21–28	21	14–21	7–28
Objects per a day	15–20	20–40	60	60	100–150	100	100	80–100
Registration	P	P–M	Mera	Mpc	PC	PC	PC	PC
1-st (ring) Reflector	S	S	A	A+F	A+F	A+F	A+F	A+F
2-nd Reflector+Cabin1	M	M	M	M	M	M	M	M

2 Observed Properties of Variable Extragalactic Objects

Figure 1 shows typical examples of strong variable spectra. A regular variations of spectra are clearly visible (see 0235+16 and 0906+01 between spectra with points marked by ‘0’ and ‘8’): a spectra disturbance (increasing or decreasing the flux) “comes” from higher to lower frequencies until it stops. The spectrum can be not variable some time in this new position. Then the situation repeats, but from the new spectrum position. It is a potentially variable again – in dependence on the variability of an accretion and the accretion part going into the jet.

Shapes of instantaneous variable spectra can be sorted to 5 main types (Kovalev et al. 2020a) in dependence on the spectral indices α ($F \propto \nu^{\alpha}$).

The structure of the observed spectra is naturally divided into two main components. “HF-component” has the maximum spectral flux density F_m of variable VLBI-compact jet at frequency ν_m more than 1 GHz. ”LF-component” has a maximum of VLBI-extended emission of the background from other part of the source – at frequencies less than 1 GHz. Its spectral indices can be equal to $-0.5 \leq \alpha < -0.1$ (“flat”-type spectrum) or $-1.0 \leq \alpha < -0.5$ (“normal”-type) or even $\alpha < -1.0$ (“steep”-type), see Popkov et al. (2020). Besides, the LF-component may be not visible if the source is very young. On the other hand, the HF-component can be not visible also — if the source is very old and, on this reason, the jet emission (“the HF-component”) is very small relative to “LF-component” because of the evolution of as accretion as the both components.

Using model analysis and statistical significance criteria, it can be shown that the observed variable spectra can be explained by the radiation of a relativistic jet in the Hedgehog model – see Kovalev et al. (2000a), Kovalev et al. (2002).

The variability in this model is offered by a variable stream of radiating particles $dN(t)/dt$ at the time moment t across a start of the jet relative to the initial stream ($dN(t_1)/dt$) at the moment $t = t_1$ (Kovalev & Larionov 1994)

$$\frac{dN(t)/dt}{(dN(t_1)/dt)} = \frac{F_m(t)}{F_m(t_1)} \left(\frac{\nu_m(t)}{\nu_m(t_1)} \right)^{(\gamma-1)/2}$$

and by the evolution of such stream perturbation during its movement along the jet in the model. The phenomenological Hedgehog model had been proposed and described by N. S. Kardashev in the editor‘s afterword to the Russian translation of the book ”Quasars” (by Jeffrey and Margaret Burbidge) fifty years ago. Its principles are very close to the well-known first model by Shklovskii (1960), Shklovskii (1965) and its nice mathematical approach by van der Laan (1966) for variable extragalactic radio source. In fact, Kardashev’s model replaced the random magnetic field of an expanding plasma cloud in Shklovsky’s model to the quasi-radial magnetic field of the jet.

By fitting several model parameters, including the angle to the observer, it is usually possible to explain the shape of the observed instantaneous spectra - up to 95% of all the studied sample objects. Examples of numerical fitting the model to spectra see in Kovalev et al. (2000a) and in Figure 2 (left panel).

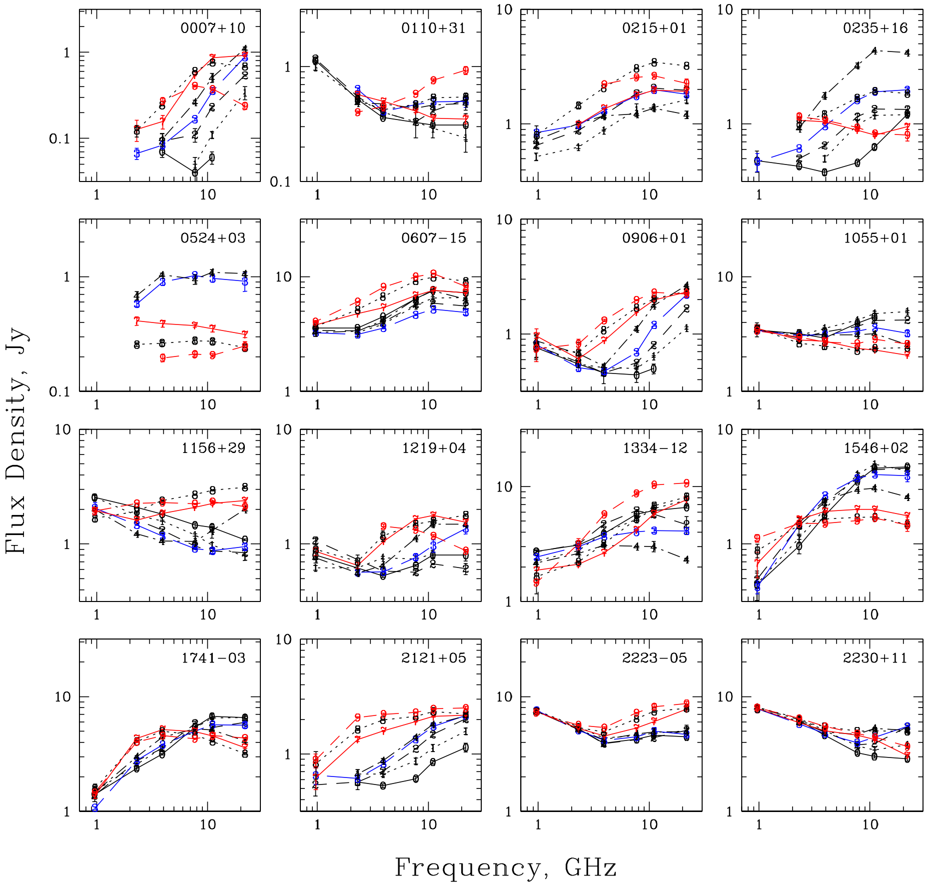

Fig. 1. Examples for selected 16 sources, RATAN-600 instantaneous spectra of which consist of one or two component with strong variability of jet emission (HF-component) in 1997-2000: 1) the LF-component is not visible in 0007+10, 1546+02, 1741−03 – "the objects are very young", 2) its contribution to the common spectrum is low relative to one of the HF-component in 0215+01, 0235+16, 2121+05 – "the sources are young", 3) contributions of the both components are approximately the same in 0110+31, 0906+01, 1055+01, 1219+04, 2223−05 – "the objects have a middle age", 4-5) "the objects are old or very old" – the LF-component is the main and the variable HF-component is visible only at 1-2 the high-frequencies or it is not visible but exist at VLBI-maps. The examples for the case 5 may be studied by Popkov et al. (2020).

3 Origin of Quasars Extreme Brightness

The conclusion on very large observed brightness temperatures of some AGNs, close to the limit of 10^{12} K for electrons, can probably be considered as the main result of VLBI for previous years. However, as it became clear from results of the *RadioAstron* project, these observed values may simply be related to the restriction on the maximum base of ground-based interferometers – by the Earth diameter. Measurements in 2012-2018 with the ground-space interferometer *RadioAstron* increased the measured values of the temperature by one-two orders of magnitude. At least the most extreme values of the brightness suggest the presence of protons in relativistic jets of these sources (Kardashev 2000).

On the other hand, active galaxies and quasars can be the sources of high-energy astrophysical neutrinos (see the next section), whose production requires processes involving relativistic protons. Invoking protons instead of electrons in the Hedgehog model described above is also extremely profitable and often necessary for the model's widespread use. The reason is the physics of operation of such a model: the energy density of the longitudinal magnetic field has to be much higher than one of the radiating particles. This may be achieved easier for protons (if relativistic protons are present in the source) than for electrons. The price of such a replacement is a strong increase of the total energy of the source.

RATAN-600 spectral data were used to improve the efficiency of VSOP (Hirabayashi et al. (2000), Kovalev et al. (2000b)) and VLBI/VLBA/VCS surveys (e.g., Petrov et al. 2005) in the search for and study of extragalactic compact structures. The spectral results helped to construct a complete sample of objects with compact jet flux densities more than 150 mJy (Kovalev et al. 2007). Today, this is the basis of the ICRF reference frame. It is also used for many astrophysical tasks including *RadioAstron*, VLBI-*Gaia*, neutrino, scattering, etc.

Spectra monitoring of 600-700 active galaxies and quasars in 2011-2018 provided data which helped optimal planning of the *RadioAstron* survey and monitoring. This included Space VLBI observations of quasars selected on the basis of flaring activity of their continuum spectra.

In the *RadioAstron* survey (Kovalev et al. 2020b):
• a record for angular resolution of 10 μas was obtained at the 1.3 cm wavelength;
• significant interferometric signal was found for about 150 AGN in 843 sessions;
• typical measured brightness temperature vary from 10^{13} K up to more than 10^{14} K, which is an order of magnitude higher than previously known values and theoretical predictions;
• the detected ultra-compact regions of extreme brightness in galaxies require a revision of our understanding of the mechanism of radiation and acceleration

of charged particles in jets. Possible mechanisms: Doppler boosting, magnetic reconnection, relativistic protons.

The joint analysis of RATAN-600 and *RadioAstron* data demonstrated the following. *RadioAstron* detects emission from ultra-compact components of quasars which preferably are in a flaring state. In this case, an increase of the RATAN-600 spectral index at high frequencies indicates beginning of the flare in the compact regions due to changes of their synchrotron opacity.

We conclude the following: 1) the extreme brightness of quasars is associated with flares and with increasing density of particles which radiate the flares; 2) increasing the Doppler factor or a reconnection of magnetic field lines is unlikely; 3) relativistic protons remain to be necessary.

4 Astrophysical Sources of High-Energy Neutrinos

Recently Plavin et al. (2020a), using VLBI data and RATAN-600 measurements in this program for 1100 variable objects over 10 years, showed the following. Quasars with higher than average radio brightness are located in the sky directions where neutrinos with energies $E > 200$ TeV, detected by the IceCube observatory, arrive from. According to the results, neutrinos from the following four strong AGN are identified with the highest probability: B 1253−055, B 1730−130, B 1741−038, B 2145+067. The RATAN-600 spectra supplemented by B 0506+056 (Kovalev et al. 2020a) in 2011–2020, September, shown in Figure 2 for the first three of them. At the time of the neutrino arrival, corresponding quasars have flares in the RATAN-600 spectra. Now this is also confirmed by other telescopes.

Published data on the "IceCube sky" for 7 years were studied by Plavin et al. (2020b). A statistical relationship between the directions to more probable neutrino event sources and AGN coordinates was found with the 3σ significance. Together with the previous analysis for energies $E > 200$ TeV, the association between radio quasars and high-energy neutrinos is established at the 4σ level: the corresponding probability of random coincidences is equal to 4×10^{-5}.

5 Summary and Prospects

RATAN-600 instantaneous spectra reflect properties of VLBI compact parsec-scale jets but it could be tricky to derive them. The developed method makes it possible to estimate flux densities from VLBI compact jets of AGNs after deducting the contribution of radiation from extended structures. Improving the accuracy of such an analysis is an immediate task. RATAN-600 spectra indicate

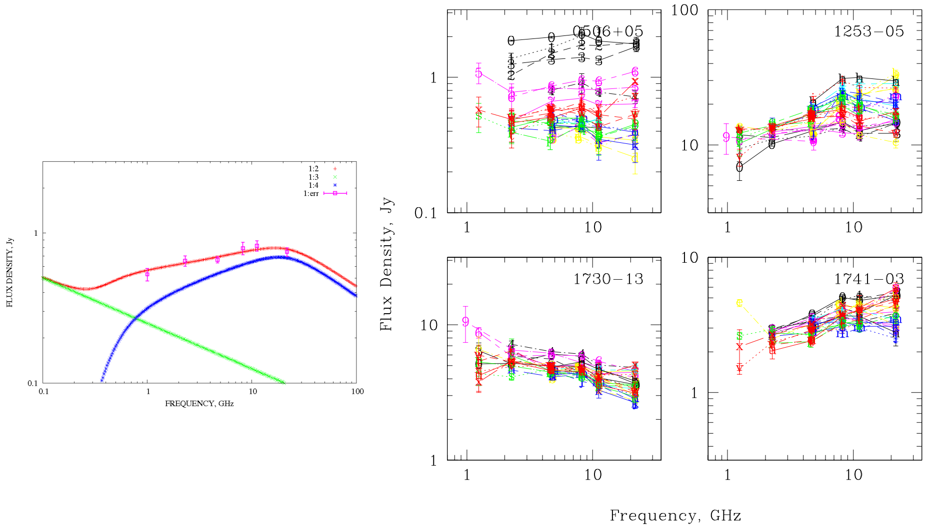

Fig. 2. *Right:* RATAN-600 instantaneous 1-22 GHz variable spectra in 2011-2020 for the radio-neutrino sources 0506+056, 3C 279 (1253−05), 1730−13 and 1741−03. They have the VLBI-bright compact jet components and are possible high-energy neutrino emitters (Plavin et al. 2020a). Their spectra are typical for the program sources (Kovalev et al. 2020a) *Left:* observed and modelled instantaneous 1-22 GHz spectrum of 0506+056 in September 2017 – near the date of the first high-energy neutrino IceCube-170922A event. RATAN-600 six points with error bars together with results of the Hedgehog jet model simulation: 1) HF-component with the maximum near 22 GHz is the VLBI compact jet emission 2) the LF-component with the maximum less than 1 GHz is the optically thin spectrum of an extended shell around the jet and 3) the resulted spectrum is equal to the sum of these components and is shown by the line across the six points data on top.

the beginning of flares in AGN cores which are found to be related to extreme brightness discovered by *RadioAstron*. RATAN-600 observes flares in quasars coincident with the arrival of high-energy neutrinos. These results indicate that synchrotron radiation of relativistic protons should be considered as a possible mechanism responsible for emission of jets in AGNs.

The open question of where and how neutrinos are born in active galaxies requires a better understanding of the connection between radio emission and neutrino events. This is being currently addressed by dedicated programs which we have started in 2020 at RATAN-600 and VLBA and is supported by neutrino data coming from the Baikal-GVD and IceCube neutrino observatories.

Acknowledgements. This program was initiated and continued at RATAN-600 thanks to a strong support by Yuri Balega, Yuri Gnedin, Nikolai Kardashev, Yuri Parijskij, and Iosif Shklovsky. It is difficult to overestimate the role of Aleksandr Berlin in laying the foundation of the low-noise multi-frequency receiver system in the mobile Cabin 1 with the secondary reflector of RATAN-600. We are thankful to Vladimir Amirkhanyan for providing us with an accurate numerical model of the RATAN-600 beam which is being continuously used many years for processing 1-22 GHz records. Observations with the SAO RAS telescopes are supported by the Ministry of Science and Higher Education of the Russian Federation. This work was supported in part by the Russian Foundation for Basic Research, grant 19-32-90140.

Bibliography

Hirabayashi, H., Fomalont, E. B., Horiuchi, S., et al. 2000, PASJ, 52, 997

Kardashev, N. S. 2000, Astronomy Reports, 44, 719

Korolkov, D. V. & Pariiskii, I. N. 1979, S&T, 57, 324

Kovalev, Y. A. 1997, Bulletin of the Special Astrophysics Observatory, 44, 50

Kovalev, Y. A., Kardashev, N. S., Kovalev, Y. Y., et al. 2020a, Advances in Space Research, 65, 745

Kovalev, Y. A., Kovalev, Y. Y., & Nizhelsky, N. A. 2000a, PASJ, 52, 1027

Kovalev, Y. A., Kovalev, Y. Y., & Nizhelsky, N. A. 2000b, in Astrophysical Phenomena Revealed by Space VLBI, ed. H. Hirabayashi, P. G. Edwards, & D. W. Murphy, 193–198

Kovalev, Y. Y., Kardashev, N. S., Sokolovsky, K. V., et al. 2020b, Advances in Space Research, 65, 705

Kovalev, Y. Y., Kovalev, Y. A., Nizhelsky, N. A., & Bogdantsov, A. B. 2002, PASA, 19, 83

Kovalev, Y. Y. & Larionov, G. M. 1994, Astronomy Letters, 20, 3

Kovalev, Y. Y., Nizhelsky, N. A., Kovalev, Y. A., et al. 1999, A&AS, 139, 545
Kovalev, Y. Y., Petrov, L., Fomalont, E. B., & Gordon, D. 2007, AJ, 133, 1236
Parijskij, Y. N. 1993, IEEE Antennas and Propagation Magazine, 35, 7
Petrov, L., Kovalev, Y. Y., Fomalont, E. B., & Gordon, D. 2005, AJ, 129, 1163
Plavin, A., Kovalev, Y. Y., Kovalev, Y. A., & Troitsky, S. 2020a, ApJ, 894, 101
Plavin, A. V., Kovalev, Y. Y., Kovalev, Y. A., & Troitsky, S. V. 2020b, ApJ submitted, arXiv:2009.08914
Popkov, A. V., Kovalev, Y. Y., Petrov, L. Y., & Kovalev, Y. A. 2020, AJ submitted, arXiv:2008.06803
Preston, R. A., Morabito, D. D., Williams, J. G., et al. 1985, AJ, 90, 1599
Shklovskii, I. S. 1960, Soviet Ast., 4, 243
Shklovskii, I. S. 1965, Soviet Ast., 9, 22
van der Laan, H. 1966, Nature, 211, 1131